Supplement of Earth Syst. Dynam., 16, 1655–1669, 2025
https://doi.org/10.5194/esd-16-1655-2025-supplement

Earth System Dynamics
Open Access
EGU

Supplement of

Eco-evolutionary modelling of global vegetation dynamics and the impact of CO_2 during the late Quaternary: insights from contrasting periods

Jierong Zhao et al.

Correspondence to: Sandy P. Harrison (s.p.harrison@reading.ac.uk)

This Supplementary contains the following tables and figures:

Table S1. Characteristics of the Last Glacial Maximum (LGM), mid-Holocene (MH) and pre-industrial (PI) Max Planck Institute Earth System Model (MPI-ESM1.2-LR; Mauritsen et al., 2019) simulations used to provide inputs for our experiments, including specified forcings.

Table S2. Regional contributions to total annual gross primary production (GPP) in the tropics, the northern extra-tropics (NET) and the southern extra-tropics (SET) in the Last Glacial Maximum (LGM), the mid-Holocene (MH) shown in the factorial experiments holding all but one variable constant.

Table S3. Gross primary production at the Last Glacial Maximum (LGM), mid-Holocene (MH) and the pre-industrial (PI) as simulated by earth system models participating in the fourth phase of the Palaeoclimate Modelling Intercomparison Project (PMIP4; Kageyama et al., 2017; Otto-Bliesner et al., 2017).

Table S4. Summary of previous factorial experiments for the Last Glacial Maximum (LGM).

Fig. S1. Change in C_4 fraction (a) at the Last Glacial Maximum (LGM) compared to the pre-industrial (PI) experiment and (b) in the mid-Holocene (MH) compared to the PI experiment.

Fig. S2. Simulated change in total annual gross primary production (GPP) between the pre-industrial (PI) and (a) the Last Glacial Maximum (LGM) and (b) the mid-Holocene (MH) as a result of holding all variables constant except climate.

Fig. S3. Simulated change in total annual gross primary production (GPP) between the pre-industrial (PI) and (a) the Last Glacial Maximum (LGM) and (b) the mid-Holocene (MH) as a result of holding all variables constant except CO_2.

Fig. S4. Simulated change in total annual gross primary production (GPP) between the pre-industrial (PI) and (a) the Last Glacial Maximum (LGM) and (b) the mid-Holocene (MH) as a result of holding all variables constant except light (photosynthetic photon flux density, PPFD).

Fig. S5. Simulated changes in (a) mean annual temperature and (b) mean annual precipitation between the pre-industrial (PI) and the Last Glacial Maximum (LGM); simulated changes in (c) mean annual temperature and (d) mean annual precipitations between the pre-industrial (PI) and the mid-Holocene (MH).

Fig. S6. Simulated change in C_4 fraction between the pre-industrial (PI) and (a) the Last Glacial Maximum (LGM) and (b) the mid-Holocene (MH) as a result of holding all variables constant except climate.

Fig. S7. Simulated change in C_4 fraction between the pre-industrial (PI) and (a) the Last Glacial Maximum (LGM) and (b) the mid-Holocene (MH) as a result of holding all variables constant except CO_2.

Fig. S8. Simulated change in C4 fraction between the pre-industrial (PI) and (a) the Last Glacial Maximum (LGM) and (b) the mid-Holocene (MH) as a result of holding all variables constant except light (photosynthetic photon flux density, PPFD).

Table S1. Characteristics of the Last Glacial Maximum (LGM), mid-Holocene (MH) and pre-industrial (PI) Max Planck Institute Earth System Model (MPI-ESM1.2-LR; Mauritsen et al., 2019) simulations used to provide inputs for our experiments, including specified forcings.

	PI	MH	LGM
Eccentricity	0.016764	0.018682	0.018994
Obliquity (°)	23.459	24.105	22.949
Perihelion -180	100.33	0.87	114.42
CO2 (ppm)	284.3	264.4	190
CH4 (ppb)	808.2	597	375
N20 (ppb)	273.0	262	200
Ice sheet	as modern	as modern	ICE6G_C
Spin-up	2000	500	3850 years after restart from previous LGM simulation
Length of simulation (yrs)	1000	500	500

Table S2. Regional contributions to total annual gross primary production (GPP, PgC yr^{-1}) in the tropics, the northern extra-tropics (NET) and the southern extra-tropics (SET) in the Last Glacial Maximum (LGM), the mid-Holocene (MH) shown in the factorial experiments holding all but one variable constant.

Region	**Time period**	**Climate**	**CO2**	**PPFD**
Tropics (25°N-25S)	LGM	-3.5	-4.7	0.2
NET (>25°N)	LGM	-11.2	-6.5	1.0
SET (>25°S)	LGM	-0.1	-1.0	0.0
Tropics (25°N-25S)	MH	0.9	-1.2	-0.5
NET (>25°N)	MH	1.5	-1.2	1.5
SET (>25°S)	MH	-0.5	-0.2	0.0

Table S3. Gross primary production (Pg C yr^{-1}) at the Last Glacial Maximum (LGM), mid-Holocene (MH) and the pre-industrial (PI) as simulated by earth system models participating in the fourth phase of the Palaeoclimate Modelling Intercomparison Project (PMIP4; Kageyama et al., 2017; Otto-Bliesner et al., 2017).

Model	**LGM**	**MH**	**PI**
MPI-ESM1-2-LR	67.8	116.9	121
AWI-ESM-1-1-LR	61.4	106.5	95
INM-CM4-8	110.7	137.5	140.6
MIROC-ES2L	108.6	146.1	151.7
NCAR.CESM2	n/a	103.8	115.0
IPSL-CM6A-LR	n/a	106.7	116.0
NorESM2-LM	n/a	123.7	134.2
ACCESS-ESM1-5	n/a	97.9	105.6
GISS-E2-1-G	n/a	106.0	121.1

Table S4. Summary of factorial experiments for the Last Glacial Maximum (LGM).

	Vegetation model	Baseline	Baseline CO_2 (ppm)	LGM CO_2 (ppm)	Index	Baseline value (Pg C $^{yr-1}$)	Climate effect	CO2 effect
This study		PI (common area)	280	190	GPP	99.1	–15%	–12%
Chen et al. (2019)	ORCHIDEE-MICT	PI (total area)	285	185	GPP	135.8	–11%	–54%
Haas et al. (2023)	P model + BIOME4	Modern (total area)	395	190	GPP	149.37	MPI: –29% AWI: –25% CESM: –41%	–55%
Martin Calvo and Prentice (2015)	LPX	PI (total area)	280	195	NPP	63.9	–2%	–23%
O'ishi and Abe-Ouchi (2013)	MIROC-LPJ	PI (common area)	285	185	NPP	54	–11%	–24%
Claussen et al. (2013)	JSBACH	PI (total area)	280	185	NPP	57.9	–4%	–45%
Woillez et al. (2011)	ORCHIDEE	Modern (total area)	310	185	NPP	TrBE: ≈570 TempNE: ≈500 TempBS:≈640 BoNE: ≈ 400 BoBS: ≈ 760	TrBE: 16% TempNE: 8% TempBS: –11% BoNE: –5% BoBS: –20%	TrBE: –68% TempNE: –62% TempBS: –39% BoNE: –72.5% BoBS: –42%

References for factorial experiments

Chen, W., Zhu, D., Ciais, P., Huang, C., Viovy, N., and Kageyama, M.: Response of vegetation cover to CO_2 and climate changes between Last Glacial Maximum and pre- industrial period in a dynamic global vegetation model, Quat. Sci. Rev., 218, 293-305, https://doi.org/10.1016/j.quascirev.2019.06.003, 2019.

Claussen, M., Selent, K., Brovkin, V., Raddatz, T., and Gayler, V.: Impact of CO_2 and climate on Last Glacial maximum vegetation – a factor separation, Biogeosci., 10, 3593- 360, https://bg.copernicus.org/articles/10/3593/2013/, 2013.

Haas, O., Prentice, I.C., and Harrison, S.P.: Examining the response of wildfire properties to climate and atmospheric CO_2 change at the Last Glacial Maximum, Biogeosci., 20, 3981-3995, https://doi.org/10.5194/bg-20-3981-2023, 2023.

Martin Calvo, M., and Prentice, I.C.: Effects of fire and CO_2 on biogeography and primary production in glacial and modern climates, New Phytol., 208, 987-994, 2015.

O'ishi, R., and Abe-Ouchi, A.: Influence of dynamic vegetation on climate change and terrestrial carbon storage in the Last Glacial Maximum, Clim. Past, 9, 1571–1587, https://doi.org/10.5194/cp-9-1571-2013, 2013.

Woillez, M.-N., Kageyama, M., Krinner, G., de Noblet-Ducoudré, N., Viovy, N., and Mancip, M.: Impact of CO_2 and climate on the Last Glacial Maximum vegetation: results from the ORCHIDEE/IPSL models, Clim. Past, 7, 557–577, https://doi.org/10.5194/cp-7-557-2011, 2011.

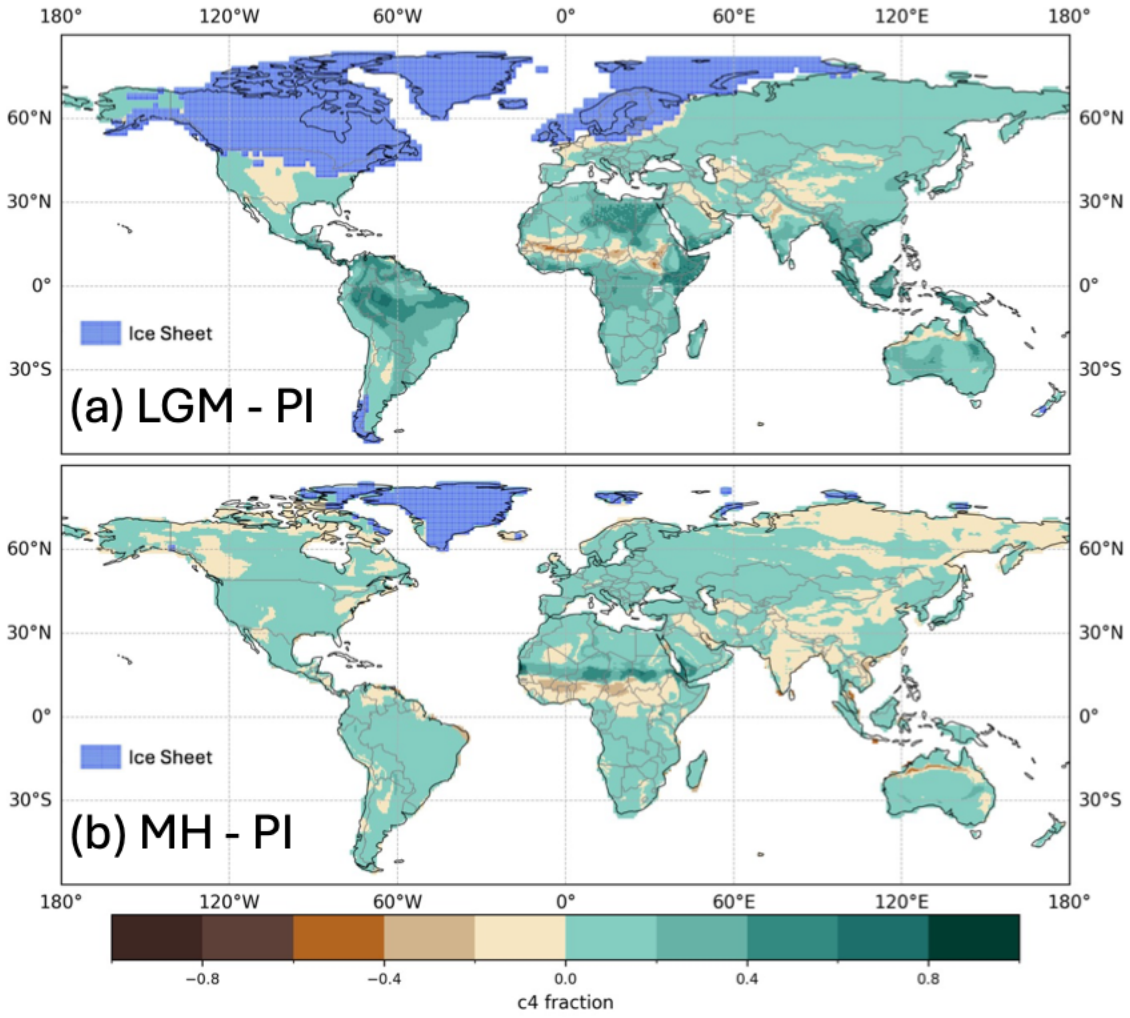

Fig. S1. Change in C_4 fraction (a) at the Last Glacial Maximum (LGM) compared to the pre-industrial (PI) experiment and (b) in the mid-Holocene (MH) compared to the PI experiment.

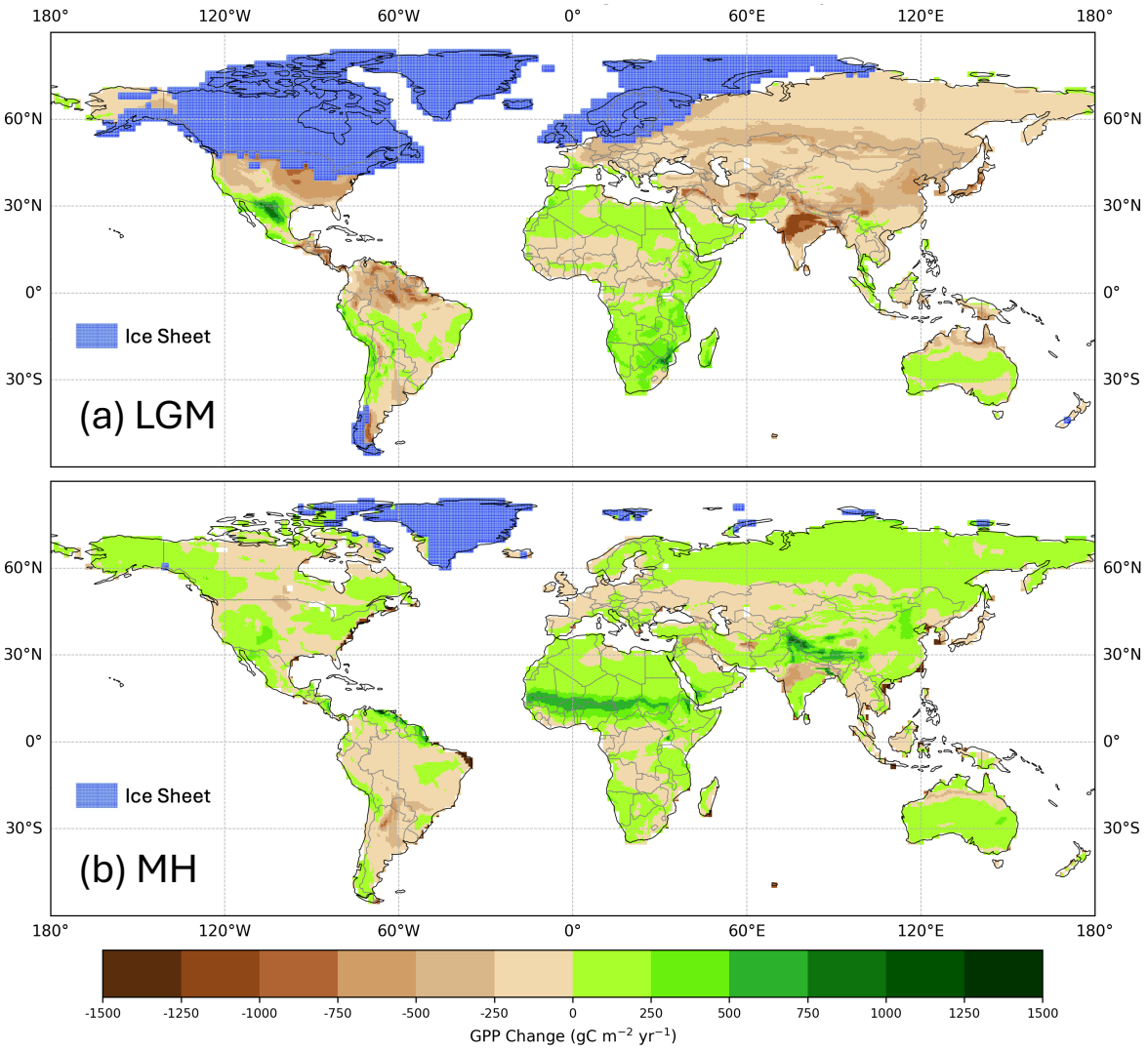

Fig. S2. Simulated change in total annual gross primary production (GPP) between the pre-industrial (PI) and (a) the Last Glacial Maximum (LGM) and (b) the mid-Holocene (MH) as a result of holding all variables constant except climate.

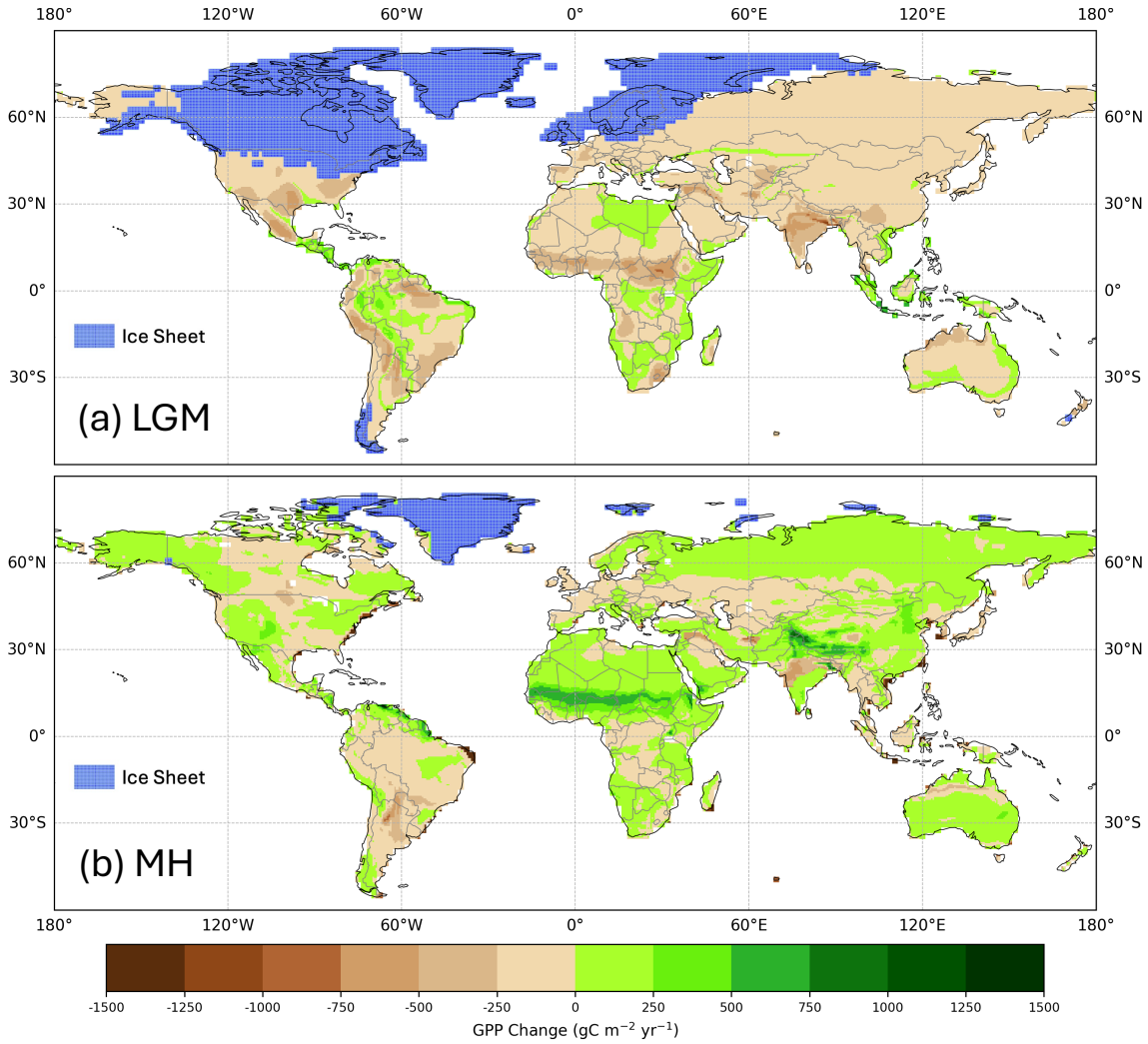

Fig. S3. Simulated change in total annual gross primary production (GPP) between the pre-industrial (PI) and (a) the Last Glacial Maximum (LGM) and (b) the mid-Holocene (MH) as a result of holding all variables constant except CO_2.

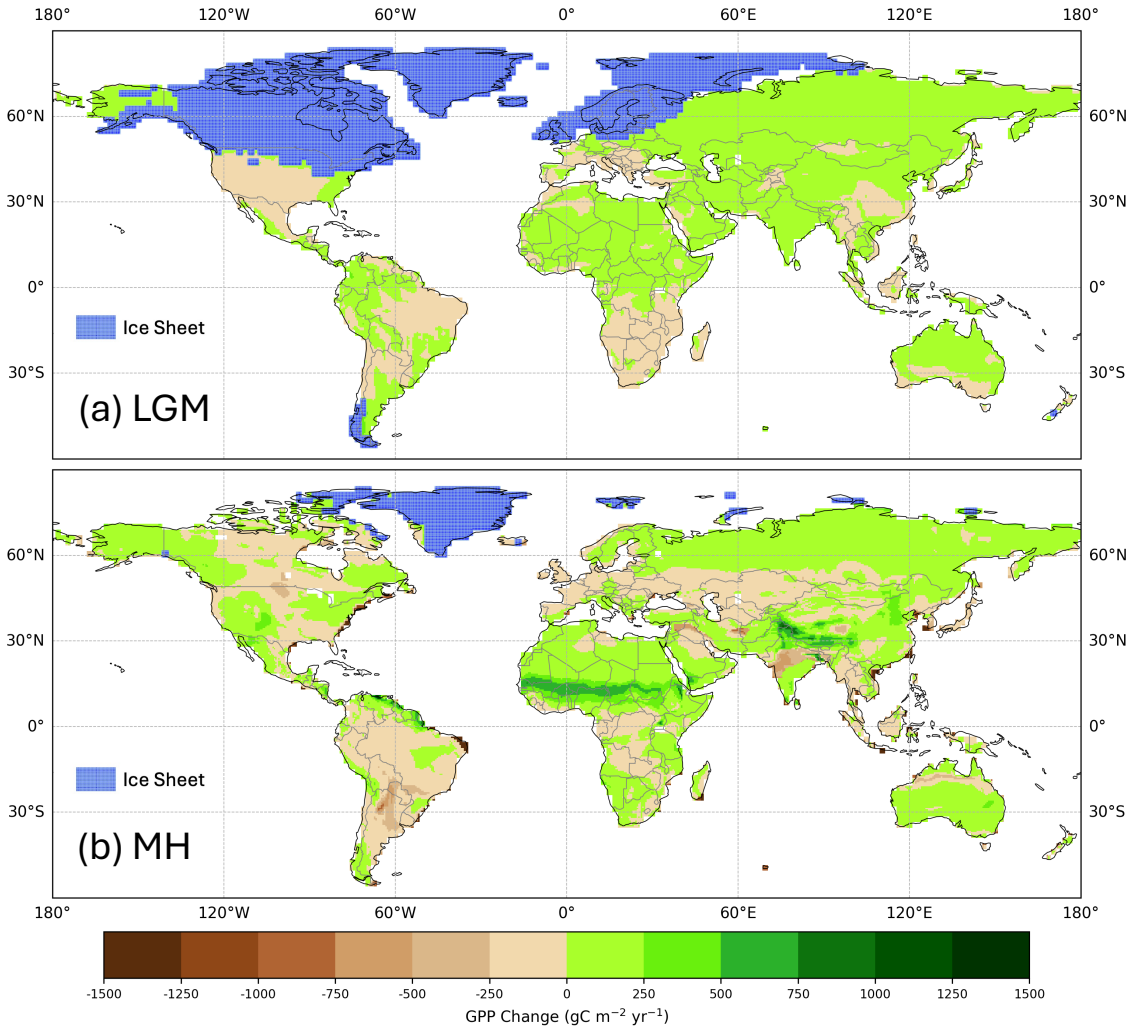

Fig. S4. Simulated change in total annual gross primary production (GPP) between the pre-industrial (PI) and (a) the Last Glacial Maximum (LGM) and (b) the mid-Holocene (MH) as a result of holding all variables constant except light (photosynthetic photon flux density, PPFD).

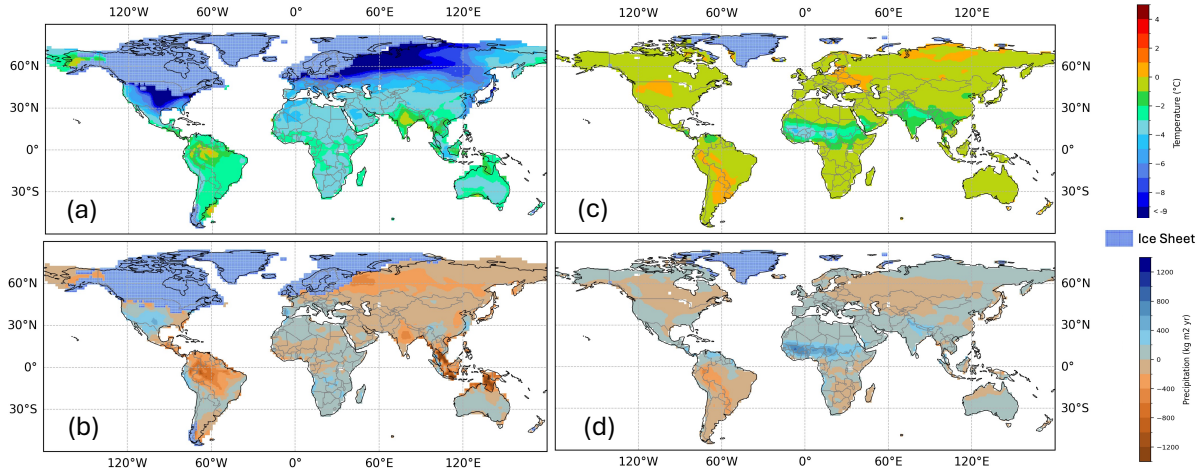

Fig. S5. Simulated changes in (a) mean annual temperature and (b) mean annual precipitation between the pre-industrial (PI) and the Last Glacial Maximum (LGM); simulated changes in (c) mean annual temperature and (d) mean annual precipitation between the pre-industrial (PI) and the mid-Holocene (MH).

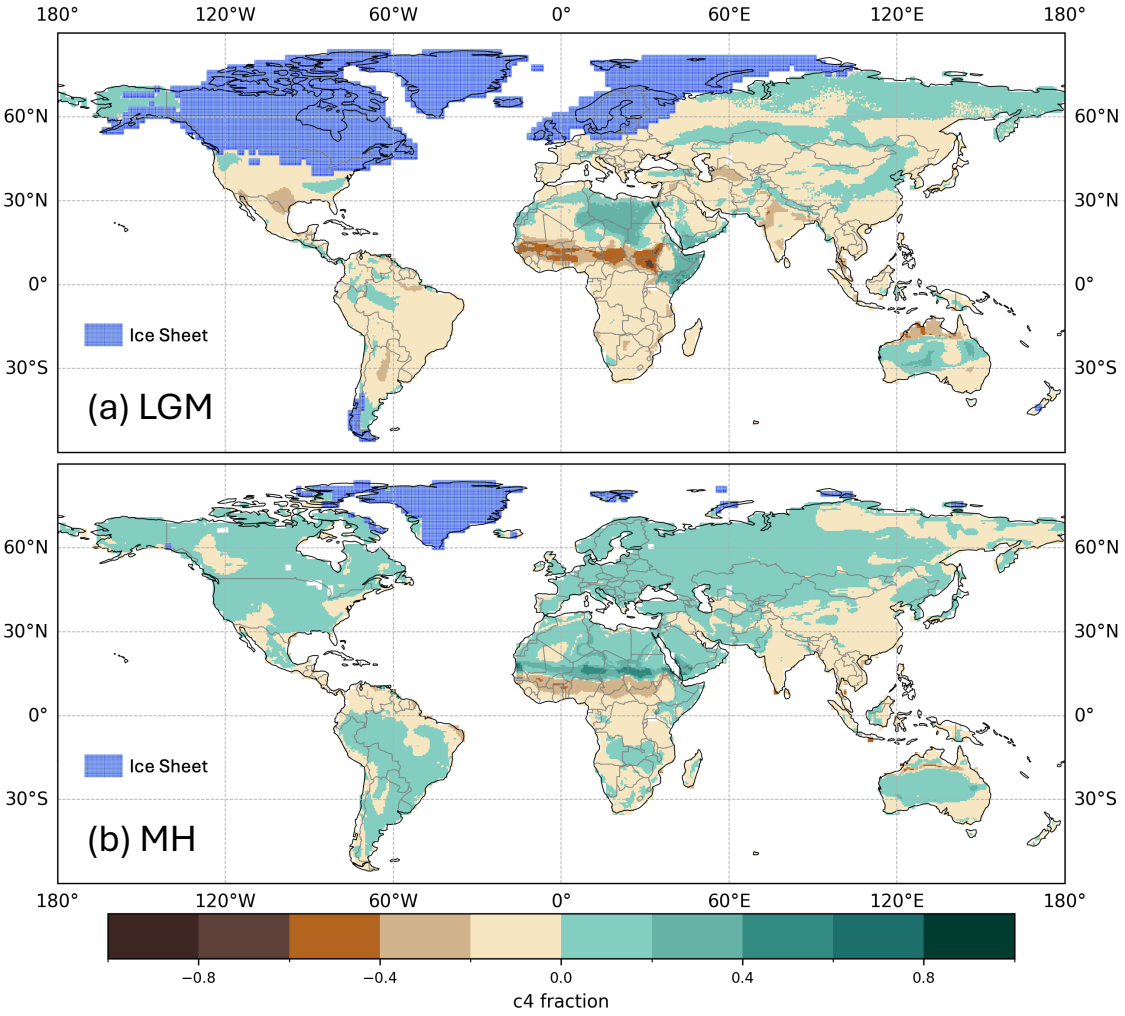

Fig. S6. Simulated change in C_4 fraction between the pre-industrial (PI) and (a) the Last Glacial Maximum (LGM) and (b) the mid-Holocene (MH) as a result of holding all variables constant except climate.

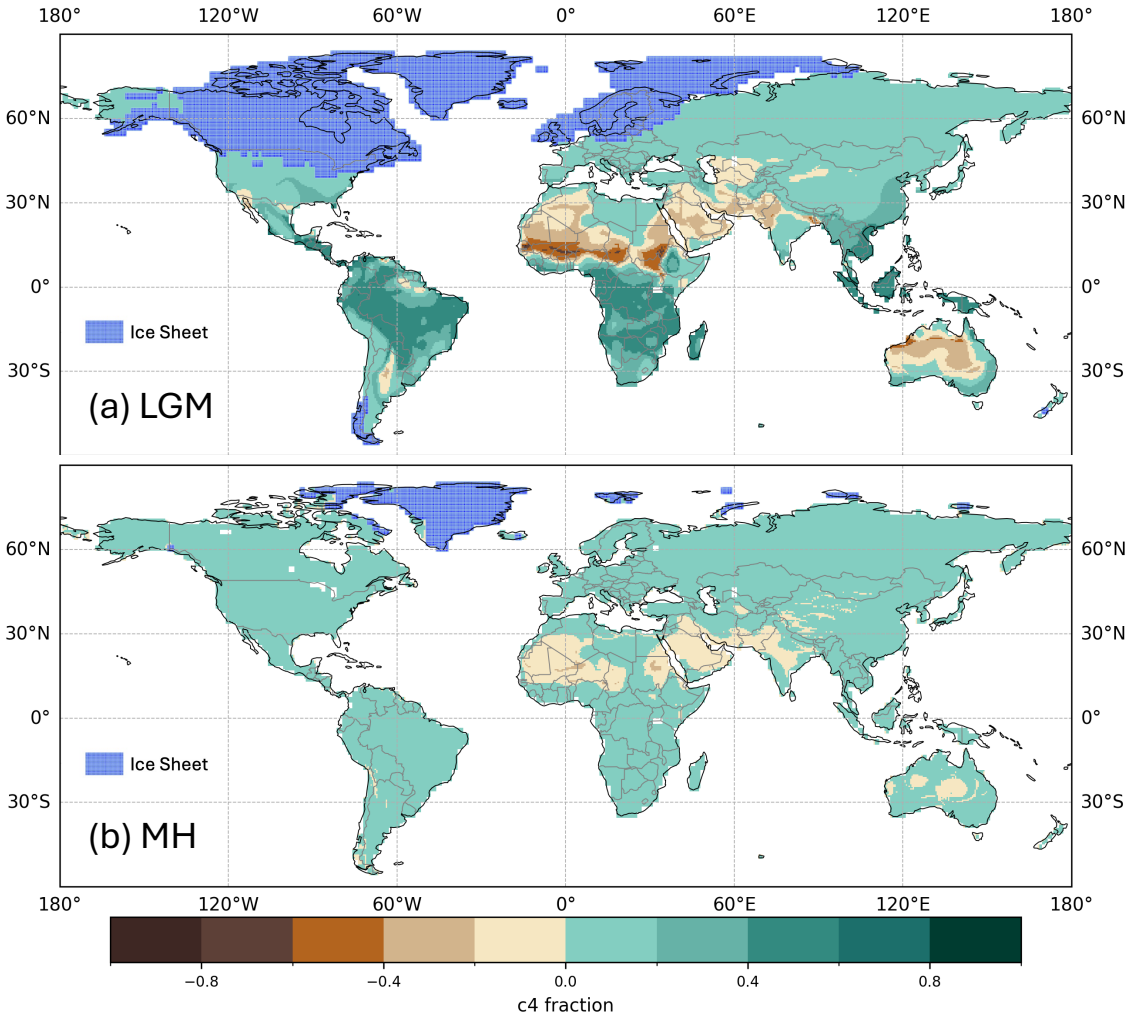

Fig. S7. Simulated change in C_4 fraction between the pre-industrial (PI) and (a) the Last Glacial Maximum (LGM) and (b) the mid-Holocene (MH) as a result of holding all variables constant except CO_2.

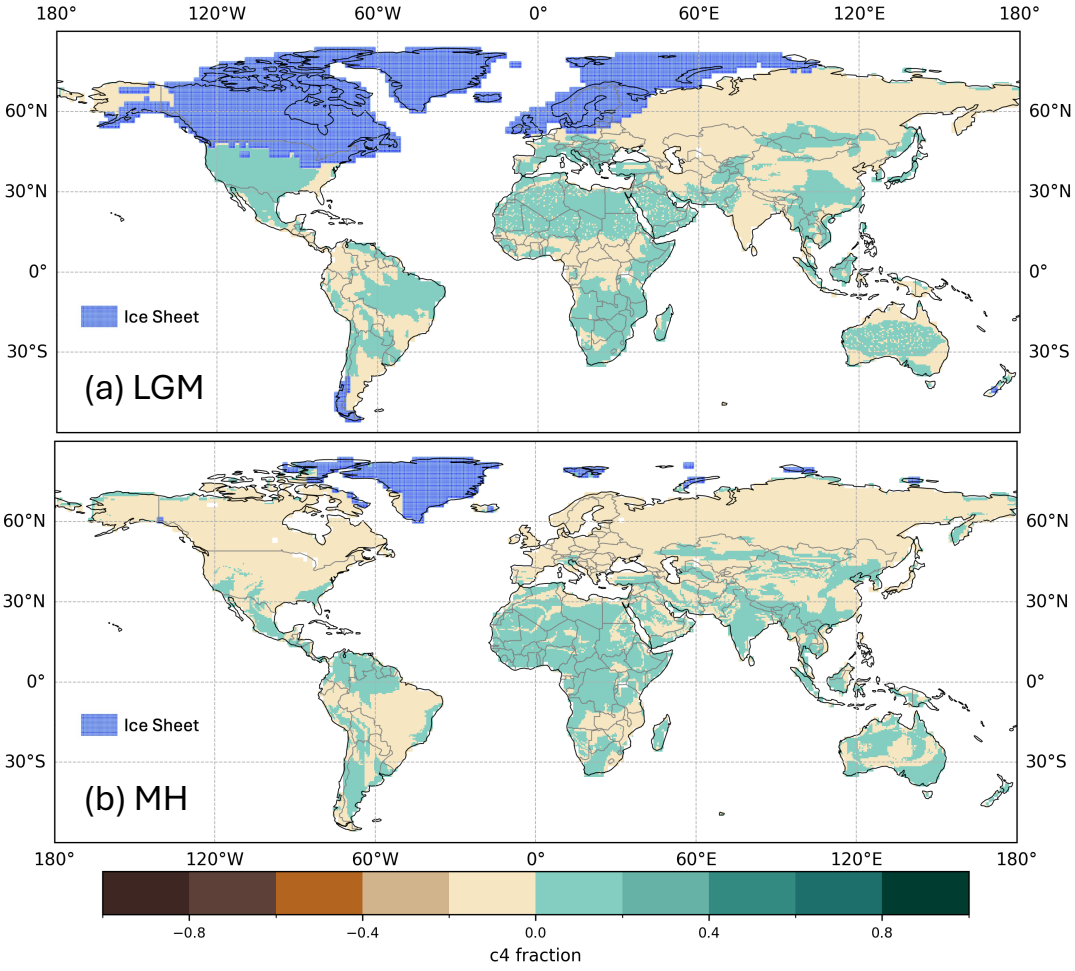

Fig. S8. Simulated change in C_4 fraction between the pre-industrial (PI) and (a) the Last Glacial Maximum (LGM) and (b) the mid-Holocene (MH) as a result of holding all variables constant except light (photosynthetic photon flux density, PPFD).

Supplementary References

Kageyama, M., Albani, S., Braconnot, P, Harrison, S.P., Hopcroft, P.O., Ivanovic, R.F., Lambert, F., Marti, O., Peltier, W.R., Peterschmidt, J.-Y., Roche, D.M., Tarasov, L., Zhang, X., Brady, E., Haywood, A.M., LeGrande, A., Lunt, D.J., Mahowald, N.M., Mikolajewicz, U., Nisancioglu, K.H., Otto-Bliesner, B.L., Renssen, H., Tomas, B., Zhang, Q., Abe-Ouchi, A., Bartlein, P.J., Cao, J., Lohmann, G., Ohgaito, R., Shi, X., Volodin, E., Yoshida, K., Zhang, X., and Zheng, W.: The PMIP4 contribution to CMIP6 – Part 4: Scientific objectives and experimental design of the PMIP4-CMIP6 Last Glacial Maximum experiments and PMIP4 sensitivity experiments, Geosci. Model Dev., 10, 4035-4055, https://doi.org/10.5194/gmd-10-4035-2017, 2017

Mauritsen, T., Bader, J., Becker, T., Behrens, J., Bittner, M., Brokopf, R., et al.: Developments in the MPI-M Earth System Model version 1.2 (MPI-ESM1.2) and its response to increasing

CO_2, J. Advan. Modeling Earth Systems, 11, 998–
1038, https://doi.org/10.1029/2018MS001400, 2019.

Otto-Bliesner, B.L., Braconnot, P., Harrison, S.P., Lunt, D.J., Abe-Ouchi, A., Albani, S., Bartlein, P.J., Capron, E., Carlson, A.E., Dutton, A., Fischer, H., Goelzer, H., Govin, A., Haywood, A., Joos, F., Legrande, A.N., Lipscomb, W.H., Lohmann, G., Mahowald, N., Nehrbass-Ahles, C., Pausata, F.S.R., Peterschmidt, J-Y., Phipps, S.J., Renssen, R., and Zhang, Q.: The PMIP4 contribution to CMIP6 – Part 2: Two interglacials, scientific objective and experimental design for Holocene and Last Interglacial simulations, Geosci. Model Dev., 10, 3979-4003, https://doi.org/10.5194/gmd-10-1-2017, 2017